This is a repository copy of *Quantifying Pelvic Periprosthetic Bone Remodeling Using Dual-Energy X-Ray Absorptiometry Region-Free Analysis.*.

White Rose Research Online URL for this paper:
http://eprints.whiterose.ac.uk/118930/

Version: Accepted Version

**Article:**

# Quantifying Pelvic Periprosthetic Bone Remodeling Using Dual-Energy X-Ray Absorptiometry Region-Free Analysis

*Andrew M. Parker,[1] Lang Yang,[1] Mohsen Farzi,[1,2] José M. Pozo,[2] Alejandro F. Frangi,[2,†] and J. Mark Wilkinson\*[,1,†]*

*[1]Department of Oncology and Metabolism, University of Sheffield, Sheffield, UK; and [2]Centre for Computational Imaging & Simulation Technologies in Biomedicine (CISTIB), Department of Electronic and Electrical Engineering, University of Sheffield, Sheffield, UK*

## Abstract

The gold standard tool for measuring periprosthetic bone mineral density (BMD) is dual-energy X-ray absorptiometry (DXA). However, resolution of the method is limited due to the aggregation of pixel data into large regions of interest for clinical and statistical analysis. We have previously validated a region-free analysis method (DXA-RFA) for quantitating BMD change at the pixel level around femoral prostheses. Here, we applied the DXA-RFA method to the pelvis, and quantitated its precision in this setting using repeated DXA scans taken on the same day after repositioning in 29 patients after total hip arthroplasty. Scans were semiautomatically segmented using edge detection, intensity thresholding, and morphologic operations, and elastically registered to a common template generated through generalized Procrustes analysis. Pixel-wise BMD precision between repeated scans was expressed as a coefficient of variation %. Longitudinal BMD change was assessed in an independent group of 24 patients followed up for 260 wk. DXA-RFA spatial resolution of 0.31 mm$^2$ provided approximately 12,500 data points per scan. The median data-point precision was 17.8% (interquartile range 14.3%–22.7%). The anatomic distribution of the precision errors showed poorer precision at the bone borders and superior precision to the obturator foramen. Evaluation of longitudinal BMD showed focal BMD change at 260 wk of −26.8% adjacent to the prosthesis-bone interface (1% of bone map area). In contrast, BMD change of +39.0% was observed at the outer aspect of the ischium (3% of bone map area). Pelvic DXA-RFA is less precise than conventional DXA analysis. However, it is sensitive for detecting local BMD change events in groups of patients, and provides a novel tool for quantitating local bone mass after joint replacement. Using this method, we were able to resolve BMD change over small areas adjacent to the implant-bone interface and in the ischial region over 260 wk after total hip arthroplasty.

**Key Words:** Bone mineral density; dual-energy X-ray absorptiometry; pelvis; total hip arthroplasty.

## Introduction

Prosthesis design influences the local mechanical environment within the surrounding bone, resulting in strain-adaptive bone remodeling *(1)*. Periprosthetic bone loss is a

risk factor for fracture and causes reconstruction challenges at revision surgery *(2,3)*. The gold standard method for measuring periprosthetic bone mineral density (BMD) is dual energy X-ray absorptiometry (DXA) *(4–6)*. A typical hip DXA scan contains over 10,000 pixel data points, including both densitometric and spatial information *(7)*. However, the resolution of conventional DXA image analysis is limited, as the anatomic location of individual pixels cannot be mapped longitudinally and between patients due to variations in patient positioning and anatomy. Pixel BMD data are aggregated into discrete regions of interest (ROIs)

to overcome this limitation, with each ROI containing data from a large set of individual pixels *(8,9)*. This analysis approach avoids the issue of pixel mapping but results in substantially reduced spatial resolution, as well as underestimating true local BMD change *(6,10)*.

Advances in image processing, nonrigid registration, and statistical parametric mapping *(11,12)* have allowed subtle spatiotemporal BMD change to be measured at pixel-level resolution around femoral prostheses *(13)*. This approach, which we have termed DXA region-free analysis (DXA-RFA), is built around a combination of principles. The first is an algorithm to extract a pixel BMD map from the DXA scans that is based upon a proprietary BMD mapping algorithm (APEX 3.2, Hologic Inc., Waltham, MA, USA) *(13)*. The second element is an image nonrigid registration method to allow the anatomic alignment of individual pixel data points between independent scans, allowing point estimates of BMD to be made across both time and between individuals. This methodology can provide BMD analysis at a resolution similar to the original scan acquisition. We have previously applied this method to quantitate BMD change around a range of femoral prostheses and to identify focal areas of BMD change adjacent to the prosthesis-bone interface *(14,15)*. In this study, we applied the DXA-RFA method to quantitate pelvic periprosthetic BMD. We quantified its precision at a pixel level and evaluated its ability to detect longitudinal pelvic periprosthetic BMD change in patients followed up for 260 wk after total hip arthroplasty (THA).

## Patients and Methods

### Participants and Scan Acquisition

All subjects had DXA scans performed after THA for idiopathic osteoarthritis. All scans were performed as part of ethics committee-approved studies, for which all subjects had provided written informed consent. Scans were acquired using a fan-beam densitometer (QDR 4500A, Hologic Inc. Waltham, MA, USA) in the metal-removal hip-scanning mode, and according to a standardized protocol *(6)*. Briefly, pelvic scan acquisition was begun 2 cm below the lower border of the inferior pubic ramus, using a field width of 15 cm. The scans were centered so that the acetabular component lay in the center of the field. The acquisition was continued proximally up to 2 cm above the lower limit of the ipsilateral sacroiliac joint.

### Data Extraction, Segmentation, and Calibration

The pelvic DXA-RFA method was implemented using MATLAB software v7.11.0.584 r2010b (Mathworks, Cambridge, MA, USA). Each scanned image was segmented into prosthesis and bone compartments using semiautomated edge detection, intensity thresholding, and morphologic operations, as described previously *(13)*. Manual oversight and input is required to identify the femoral head, adjust intensity thresholds and complete gaps in the resulting

contours. BMD at each pixel in the bone compartment was calculated using proprietary Hologic technical information under a nondisclosure agreement between the University of Sheffield and Hologic. The pixel BMD data were then scaled using a calibration factor by regression against known pixel BMDs of a European Spine Phantom extracted with the DXA-RFA algorithm and measured using Hologic APEX 3.2 software.

### Template Generation and Image Registration

A series of anatomic landmarks at the obturator foramen and femoral head were used as reference points for image alignment. A total of 108 control points were automatically located on the pelvic bone contour on the DXA image, with 29 of these defining the contour of the acetabular prosthesis. The boundaries of the scan analysis area were defined as follows. The vertical distance between the obturator foramen center and the femoral head center was defined as distance "H." The superior analysis boundary was defined as 1.6H above the femoral head, with the inferior boundary 1.2H below. The medial boundary was the most medial edge of the obturator foramen, and the lateral boundary the outer surface of the iliac wing.

A reference template was then generated using generalized Procrustes alignment *(16)*. Initially, a typical case was selected as a reference template, and each set of controlling landmarks was registered with it to remove the orientation and scale variability. Then, the template was updated with the average of registered landmark sets. The algorithm was iterated until convergence to find the reference template that best fits the series of hip shapes in the DXA images to be analyzed (Fig. 1A).

Next, each DXA scan was automatically and elastically aligned to the generated template using thin-plate splines registration controlled by the extracted anatomic landmarks *(17,18)*. The resulting transformation mapped each anatomic point on the DXA image to the corresponding position on the template (Fig. 1B), ensuring images were standardized to the reference shape with anatomic correspondence throughout all scans *(19)*.

### Evaluation of Pelvic DXA-RFA Precision

The precision of the DXA-RFA method was assessed using repeated DXA scans of the pelvis acquired on the same day after repositioning in 29 subjects (12 women), mean age 52 yr (standard deviation [SD] 9.8). Scans were acquired at a mean of 6 months (SD 3) after THA *(6)*. All patients received a hybrid replacement, with a cemented femoral component (Ultima-TPS, DePuy Ltd, Leeds, UK), and a cementless press-fit acetabular component (Plasma cup, Braun Ltd, Sheffield, UK). The analytic variability of the DXA-RFA method (algorithm, template registration, and operator variability) was assessed by repeat analysis of identical scans (58 scans in 29 patients; each scan was analyzed twice). Precision of the method in clinical practice (patient positioning, analytic and DXA hardware calibration) *(20)* was quantitated on serial DXA image
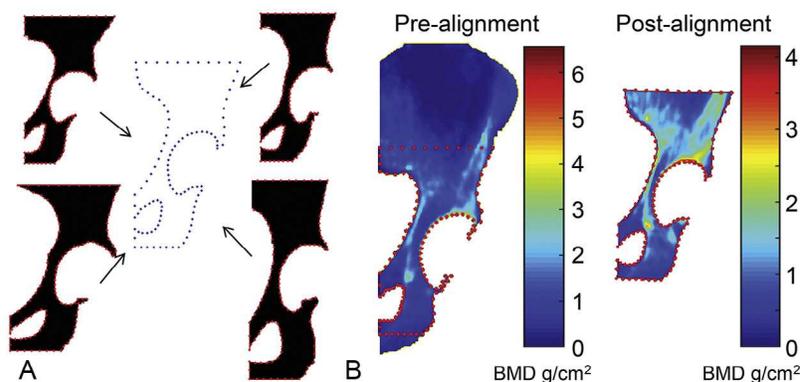
**Fig. 1.** (**A**) Landmark generation and Procrustes analysis, showing the generation of best-fit template by Procrustes analysis with 4 example scans. Control points on individual scans and master template are highlighted. (**B**) Heat map displaying bone mineral density (BMD, g/cm²) at each pixel for a singular dual-energy X-ray absorptiometry (DXA) scan before and after elastic registration to the common template.

acquisitions taken on the same day after repositioning. Clinical precision was calculated for each individual BMD data point by comparison of each pixel BMD value in the scans before and after repositioning (n = 29 pairs of scans). To quantitate the variability attributable to the segmentation process, a dice similarity coefficient was calculated *(21)*. This is a spatial overlap index, with 0 indicating no spatial overlap, and 1 indicating complete overlap. Bone compartment areas between segmentation episodes for identical scans and bone compartment areas generated at segmentation of repositioned scans were assessed, to define the variability attributable to operator variability and patient positioning, respectively.

### *Quantitating Longitudinal BMD Change Using DXA-RFA*

Quantitation of longitudinal BMD change was assessed using DXA scans acquired from the placebo group of participants in a previously reported randomized clinical trial of a single infusion of bisphosphonate (pamidronate, 90 mg) after primary THA *(22,23)*. This group comprised 24 patients (12 women), mean age 59 yr (SD 12). All patients received a hybrid replacement, with a cemented femoral component (Ultima-TPS, DePuy Ltd, Leeds, UK) and a cementless press-fit acetabular component (Plasma cup, B. Braun Ltd, Sheffield, UK), and were mobilized fully weight bearing on the first or second postoperative day. DXA scans were acquired at baseline and at weeks 6, 12, 26, 52, 104, and 260.

### *Statistical Analysis*

Precision was calculated using the International Society for Clinical Densitometry definition (ISCD precision calculator, International Society for Clinical Densitometry, Middletown, CT, USA) and expressed as a coefficient of variation (CV%) *(24)*. Longitudinal pixel-level BMD change

vs baseline was analyzed using paired *t* test to determine *p* values, and presented as a heat map of percentage BMD change vs baseline. All statistical analyses were 2-tailed, and a false discovery rate analysis was applied to control the type 1 error rate due to the multiple comparisons *(25)*. Pixels with significant BMD change are selected at $q \leq 0.05$ and the areal size of BMD change events are reported *(15)*.

### Results

#### *Precision of Pelvic DXA-RFA*

The DXA-RFA point resolution of 0.31 mm² resulted in the analysis of approximately 12,500 BMD data points per scan. The pixel-level analytic variability of the DXA-RFA method demonstrated a median pixel CV% of 6.5% (IQR 4.9%–9.2%). The overall clinical precision of the method, expressed as median pixel level CV% for the 29 pairs of repositioned patients, was 17.8% (IQR 14.3%–22.7%; Fig. 2A). The anatomic distribution of the CV%'s showed poorer precision at the bone borders and superior precision to the obturator foramen (Fig. 2B). The dice similarity coefficient in segmented bone area between the identical scans was 0.99 (IQR 0.98–1), and between repositioned scans was 0.89 (IQR 0.86–0.91).

#### *Quantifying Longitudinal BMD Change Using DXA-RFA*

Postoperative baseline BMD showed a large variation across the pelvis, with areas comprising more cortical bone proximal to the cup being of greater measured density (Fig. 3). Longitudinal measurement of BMD over 260 wk follow-up showed a gradual and consistent progression of periprosthetic BMD change (Fig. 4A–F). However, with false discovery rate correction, this only became statistically significant at week 260. At week 260 a BMD change of −26.8% (q < 0.05; Fig. 4F) was measured over a small area of the total
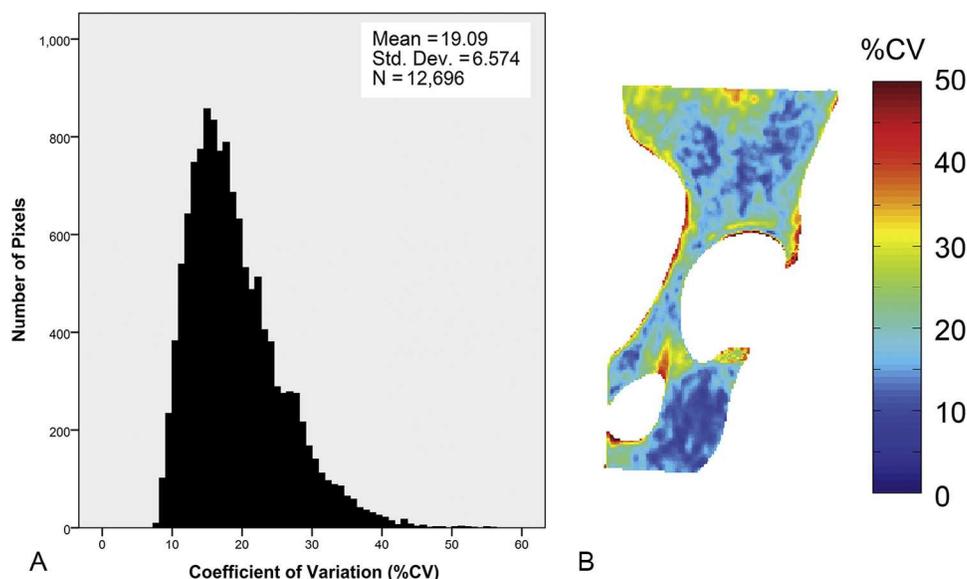
**Fig. 2.** Precision of dual-energy X-ray absorptiometry region-free analysis (DXA-RFA). Precision is expressed as coefficient of variation (CV%). (**A**) Frequency histogram showing distribution of precision values. (**B**): Anatomic distribution of precision values.
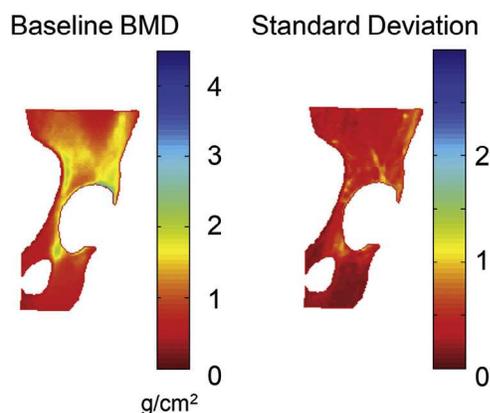


**Fig. 3.** Baseline bone mineral density (BMD) (g/cm$^2$) and standard deviation of BMD made using dual-energy X-ray absorptiometry region-free analysis (DXA-RFA).

bone map (1%) adjacent to the prosthesis-bone interface. In contrast, BMD change of +39% (q < 0.05) was observed at the outer aspect of the ischium (3% of bone map area). No other areas of significant BMD change were observed.

## Discussion

In this study, we applied DXA-RFA method to quantitate pelvic periprosthetic BMD, demonstrating that the methodology is transferable across anatomic sites, albeit with variations in precision depending on the 3-dimensional complexity of the shape involved. Using this method, we were able to anatomically resolve and quantitate pelvic BMD change at the pixel level in a group of 24 patients over 260 wk after cementless THA.

The precision of pelvic DXA-RFA was poorer than that we previously reported for the femur (13.6%, IQR 11.9%–15.6%) *(13)*. Most of the identified error was preanalytical and may be a function of between-patient anatomy and within-patient positioning variability. The semiautomatic segmentation process had a high level of repeatability between the bone areas of identical scans, and the difference in bone area between repositioned scans was modest. Pelvic tilt has been associated with reduced precision in pelvic ROI DXA analysis *(26)*. This relative imprecision of pelvic vs femoral analysis is also a feature of conventional DXA using ROI-based analysis *(6,26)*.

The distribution of longitudinal BMD changes observed is consistent with Levenston et al's Finite Element Analysis-based predictions of pelvic BMD change *(10)*. We have previously shown an increase in femoral trochanteric BMD using DXA-RFA *(15)*. Here, using pelvic DXA-RFA, we observed an increase in ischial BMD over 5 yr after THA. Both of these are sites of major muscle attachment around the hip joint: the greater trochanter for the abductor muscles and the ischium for the biceps femoris and other hamstring muscles. Horstmann et al showed increased normalized electromyographic activity over the gait cycle in both the semitendinosus and biceps femoris muscles 26 wk after THA *(27)*. As muscular activity influences local stress patterns in bone, we hypothesize that this may provide 1 explanation for the observed increase in ischial BMD in our cohort. This anatomic localization of the DXA-RFA method improves our capacity to interpret the observed BMD remodeling events as a
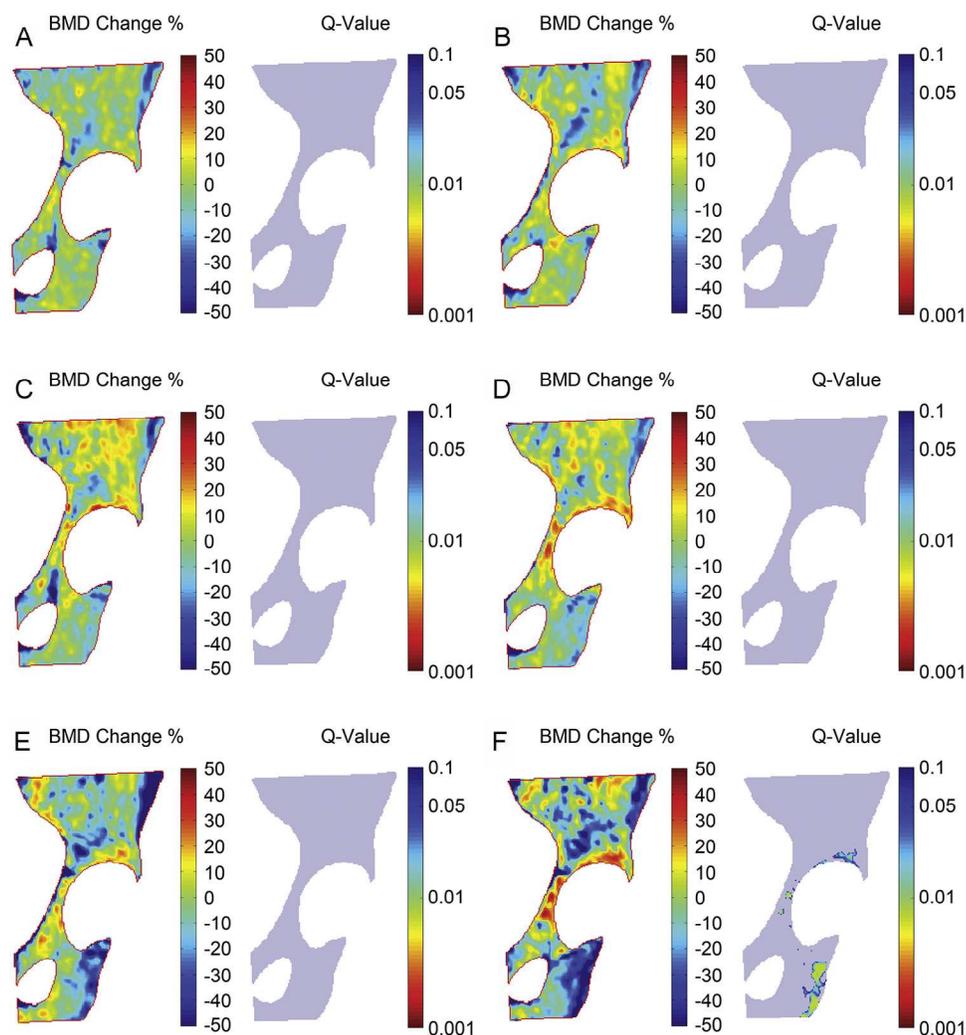
**Fig. 4.** Average postoperative bone mineral density (BMD) change and its statistical significance throughout 260 wk measured using dual-energy X-ray absorptiometry region-free analysis (DXA-RFA). The analysis is follow-up vs baseline pixel-by-pixel analysis by paired *t* test with subsequent application of a false discovery rate algorithm. BMD change is shown at the following: (**A**) 6 wk, (**B**) 12 wk, (**C**) 26 wk, (**D**) 52 wk, (**E**) 104 wk, and (**F**) 260 wk.

consequence of biological or mechanical effects that are not resolved using conventional ROI-based analysis approaches. Limitations of pelvic DXA-RFA include the morphing of individual patients' anatomic data to the common template; however, this represents a necessary compromise to enable comparison of BMD change both across time and between patients.

## Conclusions

We have adapted, validated, and applied DXA-RFA to quantitate pelvic BMD change in high resolution and using a hypothesis-free approach that is not predicated upon predefined ROIs. Despite the relatively poor pixel-level precision of the method, DXA-RFA provides temporal and spatial insight into periprosthetic BMD distribution that may inform the noninvasive clinical study of innovations in prosthetic design and surface coatings designed to modulate local BMD change and prosthesis osseointegration.

## References

1. Kerner J, Huiskes R, van Lenthe GH, et al. 1999 Correlation between pre-operative periprosthetic bone density and post-operative bone loss in THA can be explained by strain-adaptive remodelling. J Biomech 32:695–703.

2. Sheth NP, Nelson CL, Paprosky WG. 2013 Femoral bone loss in revision total hip arthroplasty: evaluation and management. J Am Acad Orthop Surg 21:601–612.

3. Cook RE, Jenkins PJ, Walmsley PJ, et al. 2008 Risk factors for periprosthetic fractures of the hip: a survivorship analysis. Clin Orthop 466:1652–1656.

4. Kröger H, Miettinen H, Arnala I, et al. 1996 Evaluation of periprosthetic bone using dual-energy X-ray absorptiometry: precision of the method and effect of operation on bone mineral density. J Bone Miner Res 11:1526–1530.

5. Kiratli BJ, Heiner JP, McBeath AA, et al. 1992 Determination of bone mineral density by dual X-ray absorptiometry in patients with uncemented total hip arthroplasty. J Orthop Res 10:836–844.

6. Wilkinson JM, Peel NFA, Elson RA, et al. 2001 Measuring bone mineral density of the pelvis and proximal femur after total hip arthroplasty. J Bone Joint Surg Br 83-B:283–288.

7. Naylor KE, McCloskey EV, Eastell R, et al. 2013 Use of DXA-based finite element analysis of the proximal femur in a longitudinal study of hip fracture. J Bone Miner Res 28:1014–1021.

8. Watts NB. 2004 Fundamentals and pitfalls of bone densitometry using dual-energy X-ray absorptiometry (DXA). Osteoporos Int 15:847–854.

9. Gruen TA, McNeice GM, Amstutz HC. 1979 Modes of failure of cemented stem-type femoral components: a radiographic analysis of loosening. Clin Orthop Relat Res 141:17–27.

10. Levenston ME, Beaupré GS, Schurman DJ, et al. 1993 Computer simulations of stress-related bone remodeling around noncemented acetabular components. J Arthroplasty 8:595–605.

11. Crum WR, Hartkens T, Hill DL. 2004 Non-rigid image registration: theory and practice. Br J Radiol 77:S140–S153. Spec No 2.

12. Ashburner J. 2009 Computational anatomy with the SPM software. Magn Reson Imaging 27:1163–1174.

13. Morris RM, Yang L, Martín-Fernández MA, et al. 2014 High-spatial-resolution bone densitometry with dual-energy X-ray absorptiometric region-free analysis. Radiology 274:532–539.

14. Wilkinson JM, Morris RM, Martin-Fernandez MA, et al. 2015 Use of high resolution dual-energy X-ray absorptiometry-region free analysis (DXA-RFA) to detect local periprosthetic bone remodeling events. J Orthop Res 33:712–716.

15. Farzi M, Morris RM, Penny J, et al. 2017 Quantitating the effect of prosthesis design on femoral remodeling using high-resolution region-free densitometric analysis (DXA-RFA). J Orthop Res doi:10.1002/jor.23536.

16. Gower JC. 1975 Generalized Procrustes analysis. Psychometrika 40:33–51.

17. Duchon J. 1976 Interpolation des fonctions de deux variables suivant le principe de la flexion des plaques minces. Revue française d'automatique, informatique, recherche opérationnelle Analyse numérique 10:5–12.

18. Meinguet J. 1979 Multivariate interpolation at arbitrary points made simple. Zeitschrift für angewandte Mathematik und Physik ZAMP 30:292–304.

19. Bookstein FL. 1989 Principal warps: thin-plate splines and the decomposition of deformations. IEEE Trans Pattern Anal Mach Intell 11:567–585.

20. Kolta S, Ravaud P, Fechtenbaum J, et al. 1999 Accuracy and precision of 62 bone densitometers using a European Spine Phantom. Osteoporos Int 10:14–19.

21. Dice LR. 1945 Measures of the amount of ecologic association between species. Ecology 26:297–302.

22. Wilkinson JM, Stockley I, Peel NFA, et al. 2001 Effect of pamidronate in preventing local bone loss after total hip arthroplasty: a randomized, double-blind, controlled trial. J Bone Miner Res 16:556–564.

23. Shetty N, Hamer A, Stockley I, et al. 2006 Clinical and radiological outcome of total hip replacement five years after pamidronate therapy: a trial extension. J Bone Joint Surg Br 88:1309–1315.

24. Baim S, Wilson CR, Lewiecki EM, et al. 2006 Precision assessment and radiation safety for dual-energy X-ray absorptiometry: position paper of the International Society for Clinical Densitometry. J Clin Densitom 8:371–378.

25. Benjamini Y, Hochberg Y. 1995 Controlling the false discovery rate: a practical and powerful approach to multiple testing. J R Stat Soc 289–300.

26. Shetty NR, Hamer AJ, Stockley I, et al. 2006 Precision of periprosthetic bone mineral density measurements using Hologic windows versus DOS-based analysis software. J Clin Densitom 9:363–366.

27. Horstmann T, Listringhaus R, Haase G-B, et al. 2013 Changes in gait patterns and muscle activity following total hip arthroplasty: a six-month follow-up. Clin Biomech (Bristol, Avon) 28:762–769.